DESIGN OF AN OPTICAL SYSTEM FOR A 5TH GENERATION, HIGH PERFORMANCE, AIR-TO-AIR MISSILE, CONSIDERING THE IMAGING PERFORMANCE DEGRADATION DUE TO THE AERODYNAMIC HEATING

Leite Junior, Paulo Roberto
Comando Geral de Tecnologia Aeroespacial (CTA)/ Instituto de Aeronáutica e Espaço (IAE)/ Divisão de Sistemas de Defesa(ASD)
DENEL Aerospace System / South Africa
prleitejunior@gmail.com

Paoli, Eduardo Tadeu
Mectron S.A./ DENEL Aerospace System/ South Africa
epaoli@ig.com.br

Hassmann, Carlos Henrique Gustavo
Mectron S.A./ DENEL Aerospace System/ South Africa
hassmann@terra.com.br

An air-to-air missile is always submitted to extreme condition of temperature, such as a hot runway over a rain forest or desert area and dropping down to very cold conditions at high altitudes. It is evident that the optical system must be able to provide satisfactory image quality under any circumstances without causing any major degradation for the image. The influence of the aerodynamic heating for this missile flying at supersonic speed must be evaluated in respect to optical performance as well. The aerodynamic heating is defined as the rise in temperature of the air adjacent to the external surface of a missile due to compression and friction during the missile flight attached to the aircraft or launched. While it appears relatively easy to calculate the aerodynamic heating, the actual wall temperature attained is the most difficult problem, and most likely a transient one. Further factors need to be included when attempting to estimate the surface temperature of a supersonic missile, such as radiation and conduction. This study investigates the interaction of these various factors and their application to the missile heating problem using classical relations provided in the literature to this type of problem allied to Computation Fluid Dynamic (CFD) techniques. The finite difference method is used to solve the resulting equations and the temperature distributions at the surface and inside the dome are obtained. Using the dome internal temperature distribution, the performance degradation of the optical system is estimated in terms of the energy focused on the detector. Due to the large temperature range, the missile optical system will experience deformation effects that will cause defocus and image degradation. A correct choice of materials, including the telescope body and dome shroud must be determined to minimize the defocus effect. Also a passive thermal compensator ought to be strategically placed to provide focus correction for all the temperature range.

Keywords: Athermalization; Optical Design; Aerodynamic Heating; Optical Compensator; Temperature Variation; Missiles

1. Introduction

The influence of the operational temperature variation for a high performance 5th generation air-to-air missile has a major effect on its optical system performance, and this effect needs somehow to be compensated in order to maintain the imaging quality under the requirements. Accordingly to the missile flight profile, the performance of the optical system may be degraded in terms of the energy ensquared on the detector, due to defocus caused by changing in the optical elements position. That occurs as a consequence of the temperature difference from –40 ^{0}C flying at 30000 feet up to +80 ^{0}C, at sea level flying at Mach 2. To accomplish the task of keeping an optical system working under these extreme conditions, a proper designed must be achieved and athermalized for that temperature range.

Another special issue is related to the detector or focal plane array (FPA). The design of the optical system must be capable to provide a perfect focus for the medium infrared (MIR) on the detector array. In this paper, two different optical systems will be designed and simulated. The first optical system will be a classic Cassegrain telescope with some modifications, using one Mangin mirror at the back and two front lenses in order to provide the correct spectral separation for the FPA. The second system will be based on a dioptric system using five IR lenses. This purely dioptric system is designed as a concept to verify and investigate its feasibility.

Once both designs are completed, the athermalization process begins by defining the worst case of temperature range for all the missile optical and mechanical components. The methodology used to define the temperature range due to the flight profile will be based on CFD (Computational Fluid Dynamic) and PSI (Parametric System Identification) with focus on the analysis of the influence of the aerodynamic heating on the dome and consequently on the optical system. The pressure distribution is obtained from CFD technique in an Euler context. From these values, the fluid flow properties are obtained from semi-empirical relations. The loss parameter associate to the heat dissipation is obtained from PSI, which uses experimental data in the identification process. The finite difference method, implemented in a context of MATLAB®, is then used to solve the resulting equations and the temperature distributions at the dome and at optical components are obtained. The next step will be based on the materials for the dome shroud and the telescope body, as well as the athermalization process following the methodology used by Kryszczynski et al.[1], although the methodology used by Tamagawa et al.[2] could be used. The main task is to keep the system performance without great degradation due to temperature variation. Finally, an analysis for the effects of stray light and ghost images will be accomplished to determine the best painting to be used on the mechanical parts as well as the best coatings for the lenses and detectors. Following all the calculations, both systems will be classified accordingly to some characteristics, including performance, and the best will integrate the missile optical system.

2. Optical Design for fhe Catadioptric and Dioptric Systems

To design both optical systems is necessary to have all the specifications and requirements in terms of field of view, f-number, energy ensquared over pixel and modulation transfer function. Some of these requirements are dependent on the focal plane size and pixel distribution. For this missile, the focal plane is constituted of one starring array matrix of 160x160 pixels, with a pixel size of 30μm. For the MIR channel, the material used will be indium antimonite (InSb). Figure 1 illustrates how the detectors and FPA are assembled as well as the cooling system.

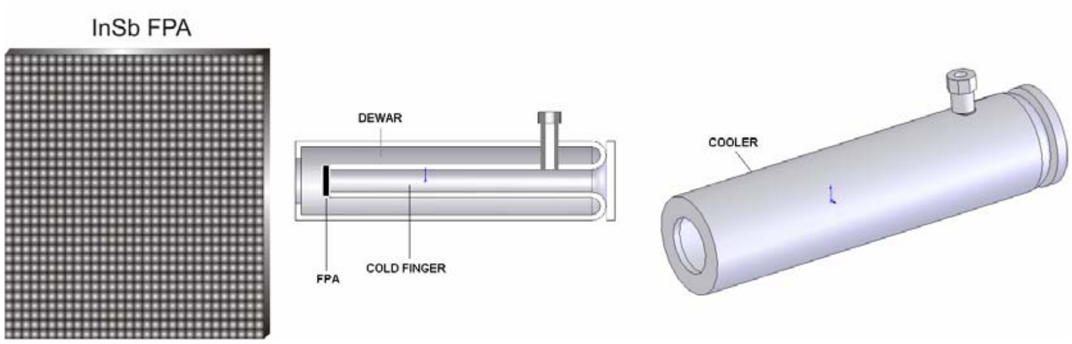

Fig. 1. Focal plane array zoomed (left), view in cut for the cooler and cold finger (right side at the top) and the full cooler (right side at the bottom).

2.1. Optical design for the catadioptric system

For the catadioptric system, the desirable field of view is $2{,}80^0$, f-number close to 1,5 and focal length equal to 98,22mm. Besides, the optical system must be close to diffraction limit for the MIR channel and the ensquared energy over pixel must be greater than 80% for full field. In terms of vignette, not more than 30% of the rays may be clipped. To accomplish this design, some refractions elements are necessary to provide the correct spectral focus and improvement of performance. The initial concept was based on a front doublet, a rear Mangin mirror, a curved secondary mirror and a last correction lens. A lay-out is shown on Figure 2.

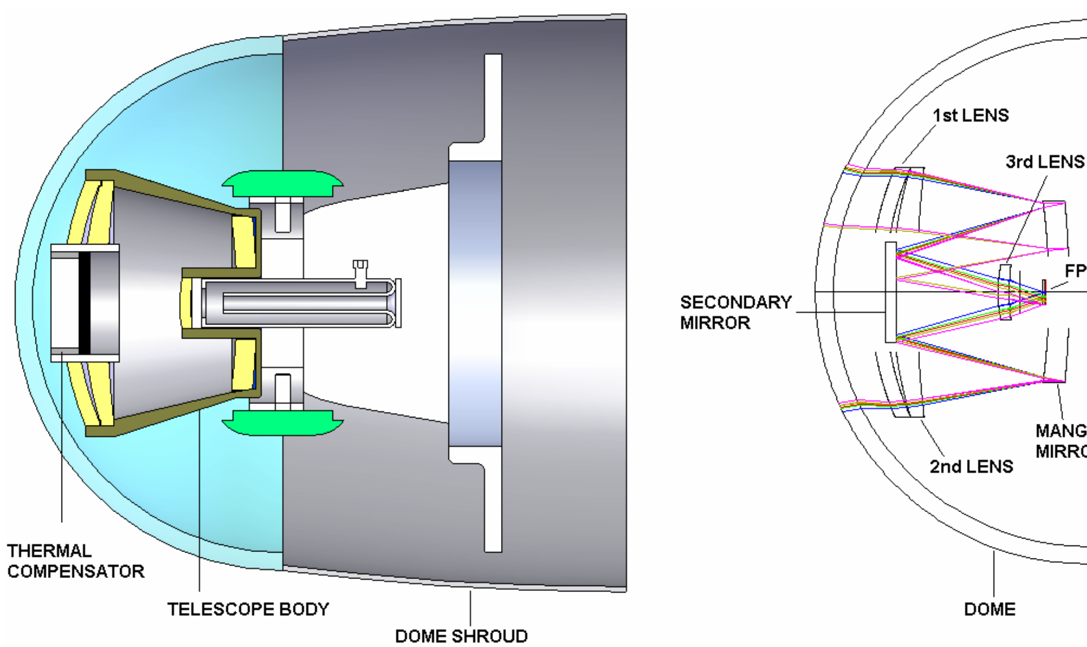

Fig. 2. Lay-Out for the catadioptric system. To the left, a full view in cut for the gimbal system including the telescope body and the thermal compensator. To the right, a diagram with the optical elements only.

The software used to design and optimize the system was ZEMAX®. The merit function used to optimize the system was based on the spot radius and all the mechanical restrictions were defined to keep the design under determined dimensions to allow the system to accomplish the requirements for movements in pitch (± 10^0) and yaw (± 90). In terms of performance, Figure 3 shows the graphics for the MTF and a full plot of the ensquared energy over field for the MIR channel. The plot for the ensquared energy over field will provide a measurement of the optical system ability to focus the available energy, considering the diffraction effects, on the focal plane array. The results show that the system is very close to diffraction limit in terms of its MTF and the ensquared energy is over 80% for full field.

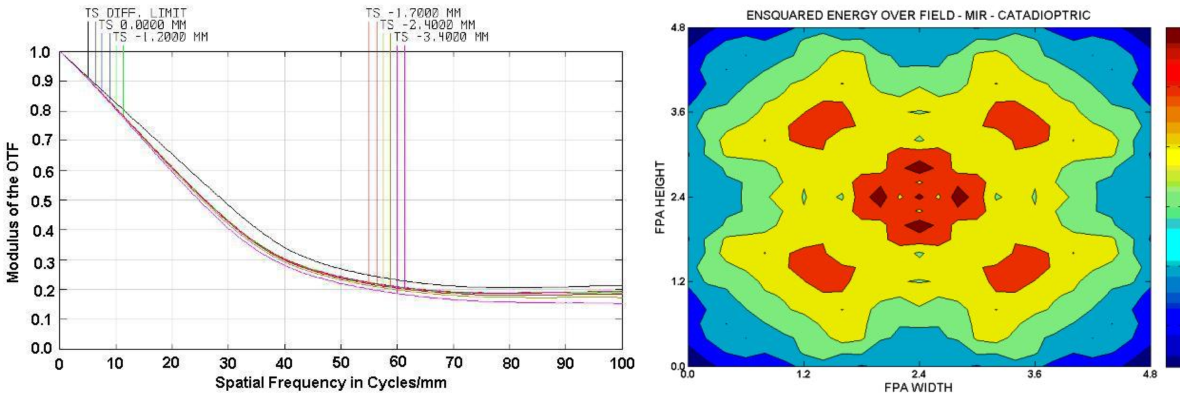

Fig. 3. To the left, the plot for the MTF. To the right, the plot for the Ensquared Energy over Field

2.2. Optical design for the dioptric system

For the dioptric system, the desirable field of view is slightly wider than $2{,}80^0$, because the requirement for the focal length is 90mm. The focal length is shorter due to mechanical restrictions because a shorter focal length generally provides a shorter mechanical system. The requirement for f-number is increased to 1,72 due to the intrinsic difficulties to design a dioptric system with an excessively large aperture. Again, the optical system must be close to diffraction limit for the MIR channel and the ensquared energy over pixel greater than 80% for full field. For this design, five lenses distributed all over the extension of the telescope were used to provide the correct spectral separation and achievement of performance. A lay-out is shown on Figure 5.

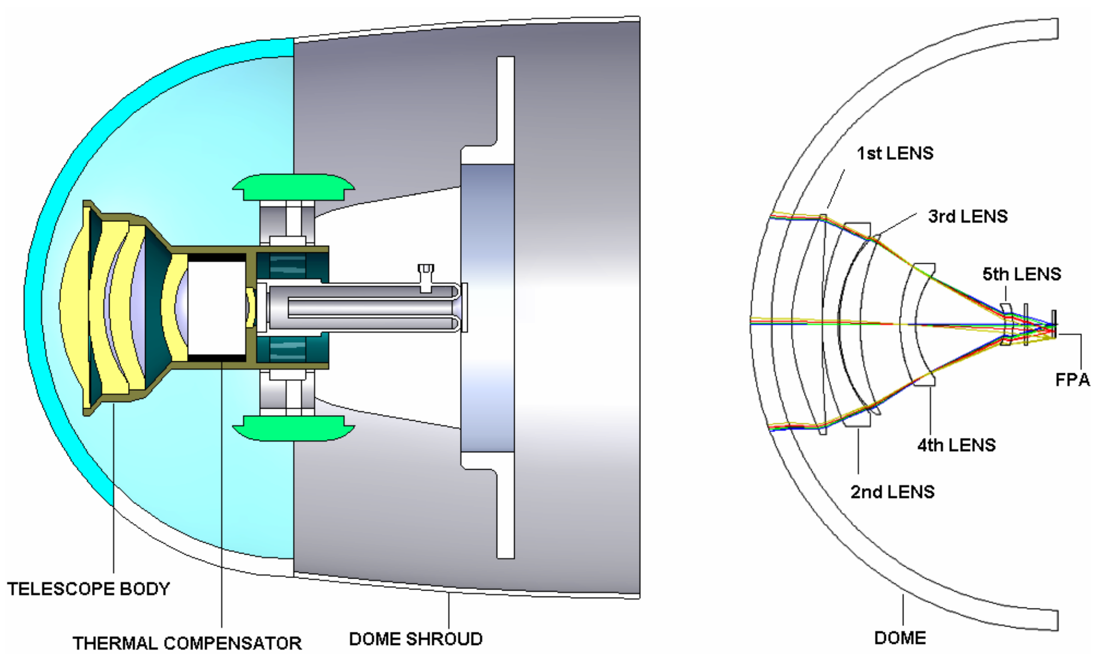

Fig. 5. Lay-Out for the Dioptric system. To the left, a full view in cut for the gimbal system including the telescope body and the thermal compensator. To the right, a diagram with the optical elements only.

The software used to design and optimize the system was also ZEMAX® and the merit function used to optimize the system was based on the method rectangular array, which tries to fit as many rays as possible into the pupil of the system. The mechanical restrictions were defined to keep the design under determined dimensions, specially the length, to allow the system to accomplish the requirements for movements in pitch ($\pm 10^0$) and yaw ($\pm 90^0$). In terms of performance, Figure 6 shows the graphics for MTF and a full plot of the ensquared energy over field for the MIR. For this dioptric system, the performance achieved was not as good as the catadioptric system, as can be seen by the MTF plot and the ensquared energy over field.

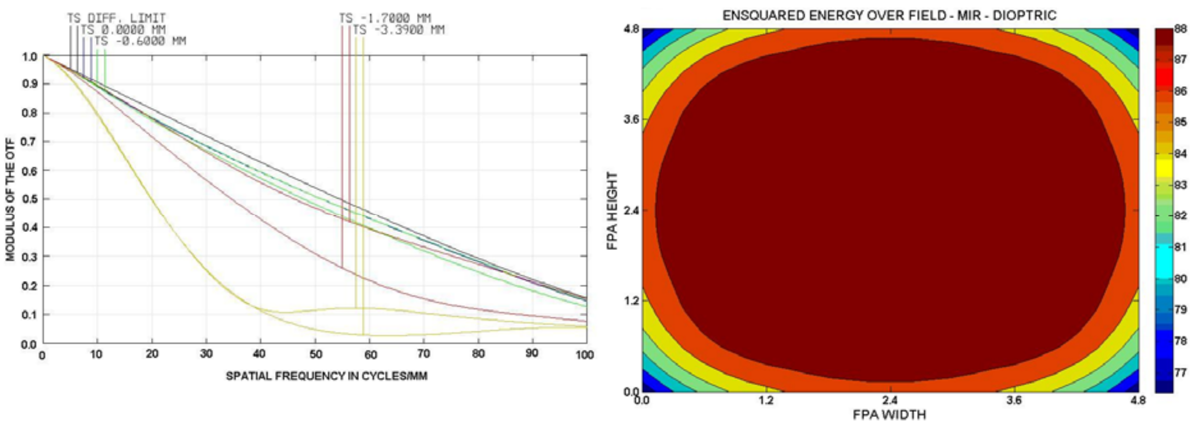

Fig. 6. To the left, the plot for the MTF. To the right, the plot for the Ensquared Energy over Field

3. Determination of the Temperature Operational Range

3.1. Temperature at Dome Surface

One of the most important requirements to design an optical design is to determine the operational range in terms of gradient of temperature 2. In the case analyzed here, the optical elements temperature can vary from -40^{0}C up to 80^{0}C to the inner elements and from -40^{0}C to 290^{0}C to the external wall of the dome. Under so critical circumstances, it is very difficult to achieve a very good optical performance. However, it will be shown that on choosing the correct method and materials for athermalization, it is possible to keep the performance under the parameters specified.

There are many complexities involved in the mathematical modeling of thermal transient at the missile dome. A variety of factors affect the skin temperature and they are not all equally important. Some of the factors affecting the missile skin temperature are: heat transfer due to forced convection; external radiation from the skin and atmospheric radiation to the skin; conduction along the skin; solar radiation to the skin; near-field radiation from hot gases, such as the hot gas cap around the missile nose; internal radiation to and from the skin; conduction through the skin; internal convection from the skin; forced cooling or heating. In this work, the influence of the solar radiation to the skin, the near-field radiation from hot gases, the internal radiation to and from the skin, the internal convection from the skin and the forced cooling or heating was considered implicitly by the use of PSI method.

3.2. Internal temperature

The mathematical formulation to determine the temperature inside of the missile front section is based on “lumped parameters” method and experimental data. In this work, the main objective is to generate the worst thermal scenarios for the optical system and it is not aimed to define the exact temperature of dome and optical components.

3.3. Numerical Implementation

Essentially, the algorithm applied to solve the mathematical model developed for the aerodynamic heating of a supersonic missile dome is based on the PSI method. The steps involved in this process are shown bellow:

Input:

Initial conditions in term of temperature and the initial guess for heat flux;
Geometry of dome indicating the laminar and turbulent regions;
Physical properties of missile front section (dome and optical system);
Pressure distribution on the dome (CFD results);
Flight profile from the flight dynamics (carriage flight);
Temporal variation of experimental temperature.

The next step is to describe the algorithm.
1- Calculate local Mach number at the edge of boundary layer based on the flight profile;
2- Calculate stagnation temperature during the flight;
3- Calculate recovery temperature in all regions on the dome;
4- Determine the wall equilibrium temperature and the temperatures at the internal components of the optical system using an estimated value for heat flux;
5- With the heat flux and the internal temperature of the components, it is possible to estimate the value for the temperature of air inside of dome;
6- Go to the step 2;
- Output
  The wall equilibrium temperature;
  The temperatures at the internal components of the optical system;
  The temperature of air inside of dome;
  The average heat flux inside of dome;

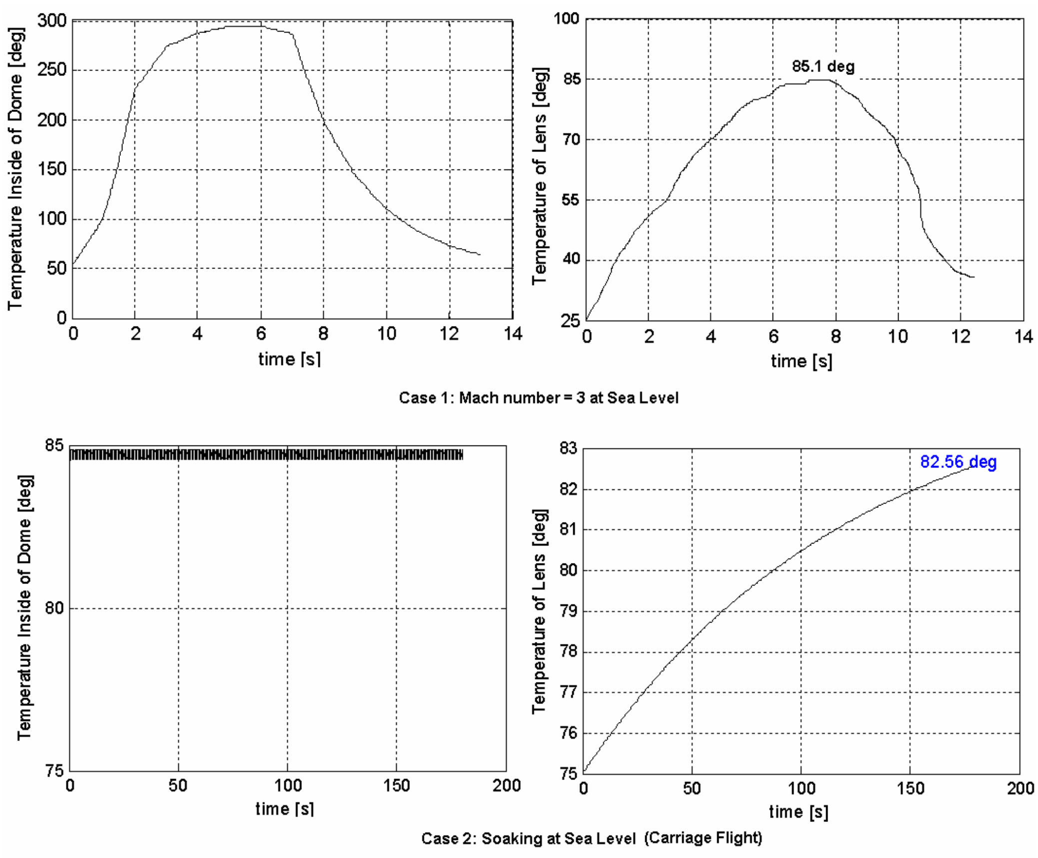

Figure 7 – Two different flight profiles for the missile and the temperatures involved

4. Athermalization of the optical systems

After the definition of the flight profile and the temperature worst cases submitted to the missile, it is necessary to athermalize both systems in order to keep the performance under the requirements. The method used will be passive athermalization combining materials of different coefficients of thermal expansion (CTE) to keep the focal plane as close as possible to its original position. The methodology utilized will be based on the implementation of thermal configurations in ZEMAX® and on the definition of a new merit function to accomplish all configurations. Five thermal configurations will be determined for MIR.

4.1. Athermalization of the catadioptric system

The athermalization process will begin for the catadioptric system. First of all, it must be defined the thermal configurations to be optimized. Table 1 illustrates the profile for five different temperature configurations.

The next step is to implement these configurations in ZEMAX® and remove all variables of the system, replacing new variables on the CTE column for the materials. A dummy surface is defined in the gimbal rotation center, the place where the telescope fits into the gimbal mechanism and will be considered the reference for all the others surfaces. For this catadioptric design, the dome shroud will be made in aluminium, the telescope body, the rings for the first and second frontal lenses and the secondary mirror barrel will be made in titanium. The dome will be made in sapphire, the first lens in CaF_2, the second lens will use Cleartran®, the mangin mirror will be made in AMTIR-1®, the secondary mirror substrate will be made in Zerodur® and finally, the last lens will use Cleartran® again. There will be one ring behind the secondary mirror that will work as a differential expansion mechanisms and the CTE for this ring material will work as a variable in the optimization process. To complete the optimization process, a new merit function will be defined accomplishing all the ten configurations defined (five for MIR and five for NIR). At Figure 2 it is possible to see the compensator.

Table 1. Thermal configurations to be optimized for the catadioptric system

Optical Components	Temp. Profile 1 Lab. Environment	Temp. Profile 2 Cold (Static)	Temp. Profile 3 Soaking (Sea Level)	Temp. Profile 4 (High altitudes, slow)	Temp. Profile 5 (Sea level, high mach number)
Dome	20^0C	-40^0C	82.56^0C	-45^0C	290^0C
First lens	20^0C	-40^0C	82.56^0C	-42^0C	85.1^0C
Second lens	20^0C	-40^0C	82.56^0C	-42^0C	85.1^0C
Mangin Mirror	20^0C	-40^0C	82.56^0C	-42^0C	85.1^0C
Field lens	20^0C	-40^0C	82.56^0C	-42^0C	85.1^0C
Detector window	20^0C	-40^0C	82.56^0C	-42^0C	85.1^0C
Cold Shield	20^0C	-40^0C	82.56^0C	-42^0C	85.1^0C
Cold Finger rear	$\leq -195^0$C	$\leq -195^0$C	$\leq -195^0$C	$\leq -195^0$C	$\leq -195^0$C

Once this new setup has been designed, the optimization process begins and after some cycles, the value for the ring CTE was found. The ring must have a CTE of 75 $^0C^{-1}$ and a length of 28mm. A good material candidate comprising this CTE is Delrin® (acetal) with a CTE approximately of 85 $^0C^{-1}$. Of course, the ring must be slightly shorter due to the difference in terms of the CTE. It is important to notice that in the simulation, the value for CTE obtained was negative, what means that the ring must be placed on the opposite side to push the mirror to the correct direction.

After the system athermalization, a tool from ZEMAX® called Image Simulation is then used to determine if there was variation in performance for all the thermal configurations. Figure 8 shows three images obtained for the Profile 1 (20^0C), Profile 4 (-42^0C) and Profile 5 (Dome at 290^0C and lenses at $85,1^0$C). As can be observed, the three images seem to be exactly the same, what means that a good optical athermalization was achieved.

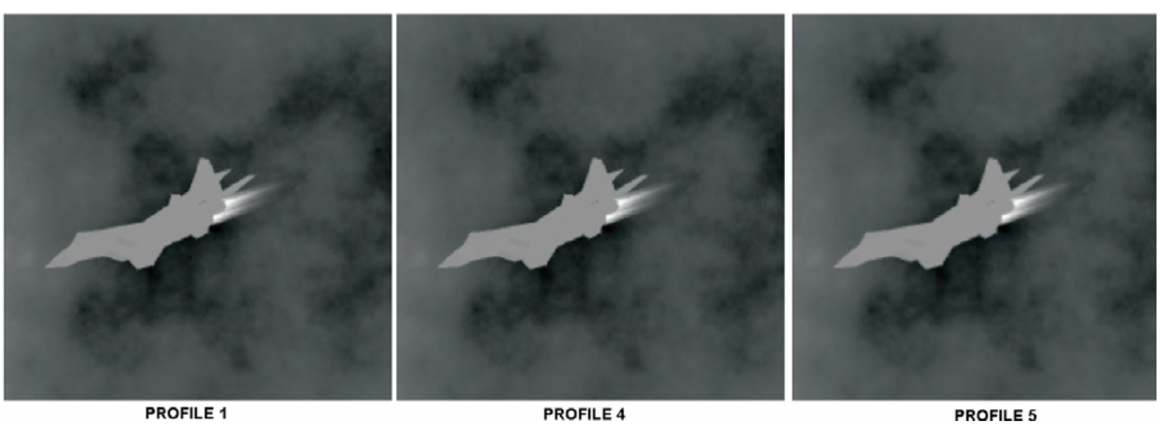

Fig. 8. Image Simulation for Profile 1, Profile 4 and Profile 5.

4.2. Athermalization of the dioptric system

The athermalization process for the dioptric system will follow the same procedure. First of all, it must be defined the thermal configurations to be optimized. As the methodology is the same, the temperatures profiles will be the same and all the lenses and dome temperatures will also follow the values describe in Table 1.

Again, the next step will be the implementation of these configurations in ZEMAX® and remove all variables of the system, replacing new variables on the CTE column for the materials. A dummy surface is also defined in the gimbal rotation center. For this dioptric design, the dome shroud will also be made in aluminium, the telescope body and the rings for all the lenses (except the ring for the fourth lens) will be made in titanium. The dome will be made in MgF_2, the first lens will use Cleartran®, the second lens cadmium selenide (CdSe), the third lens will be made of zinc sulphide (ZnS), the fourth lens will be using magnesium oxide (MgO) and the fifith lens will use silicon (Si). There will be only one ring behind the fourth lens and that will work as a differential expansion mechanism and the CTE for its material will work as variable in the optimization process. To complete this process, a new merit function will be defined accomplishing all the ten configurations defined (five for MIR and five for NIR). The diagram of Figure 4 exhibits the position for the compensator.

The ring that holds the fourth lens must have a CTE of 110^0C^{-1} and a length of 21.8mm. The material that might have such a CTE can be an acetal, although this value for the CTE is excessively high. Once more it is important to notice that in the simulation, the value for CTE obtained was negative, what means that the ring must be placed on the opposite side to push the lens to the correct direction. As can be seen from Figure 9, the three images appear again to be the same, what means that the requirements were accomplished for the most critical conditions.

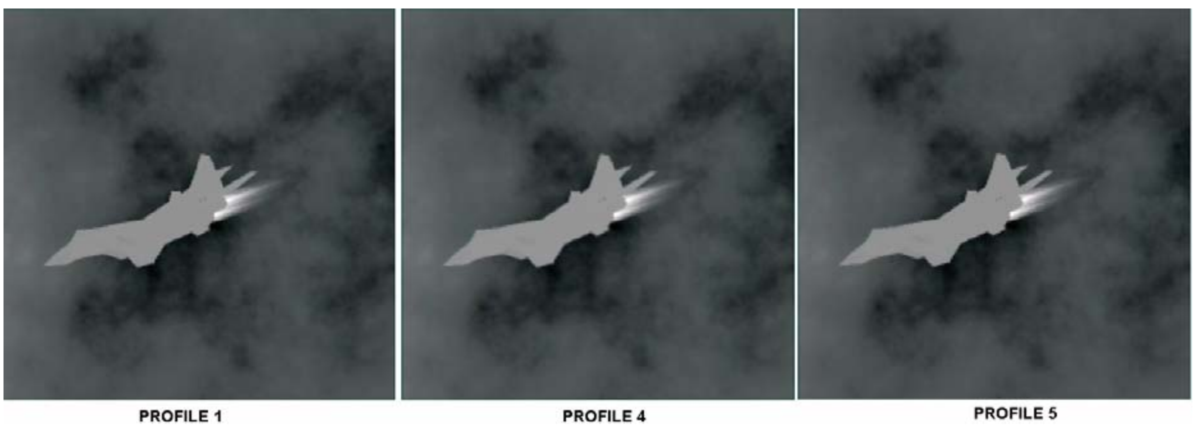

Fig. 9. Image Simulation for Profile 1, Profile 4 and Profile 5.

5. Stray Light Analysis

The final step is to determine the influence of stray light in both optical systems. The stray light analyses will be useful to determine the ability of both optical systems to reject light that is outside their instantaneous field of view (IFOV).

5.1. Stray light analyses for the catadioptric system

The requirements for stray light analyses will be rejection of energy that is at more than 5^0 away from the IFOV. The model to be used for internal reflections in the telescope body and all the holders will be a Lambertian with 100% of reflection. Naturally all the mechanical components will be painted using Nextel® to assure a very low level of internal reflectance. An IGES 3D could be used for this model 4, however, it is used ZEMAX® due to its simplicity.

To achieve the stray light model in ZEMAX®, the purely non-sequential mode had to be activated, to allow a more realistic model, where the rays can be reflected and refracted many times. Some of the mechanical parts were also modeled, specially the telescope body plus two sources of radiation, one at the IFOV and the other one tilted at 5^0. Figure 10 illustrates the model used for the stray light simulation.

One of the main advantages of the non-sequential mode is the possibility to implement the FPA with all the pixels. That will provide results even more realistic, where it is possible to check, pixel by pixel, the effects of stray light. For this catadioptric system, it is possible to observe in Figure 11 that when the two sources are simulated, some pixels that are outside of the IFOV receive some energy. However, as the energy levels of these pixels are much lower than the pixels related to the central source, the imaging processor will understand this as noise and will simply neglect their influence. Therefore, it is possible to say that this catadioptric system is able to reject stray light at 5^0 or more away from its IFOV.

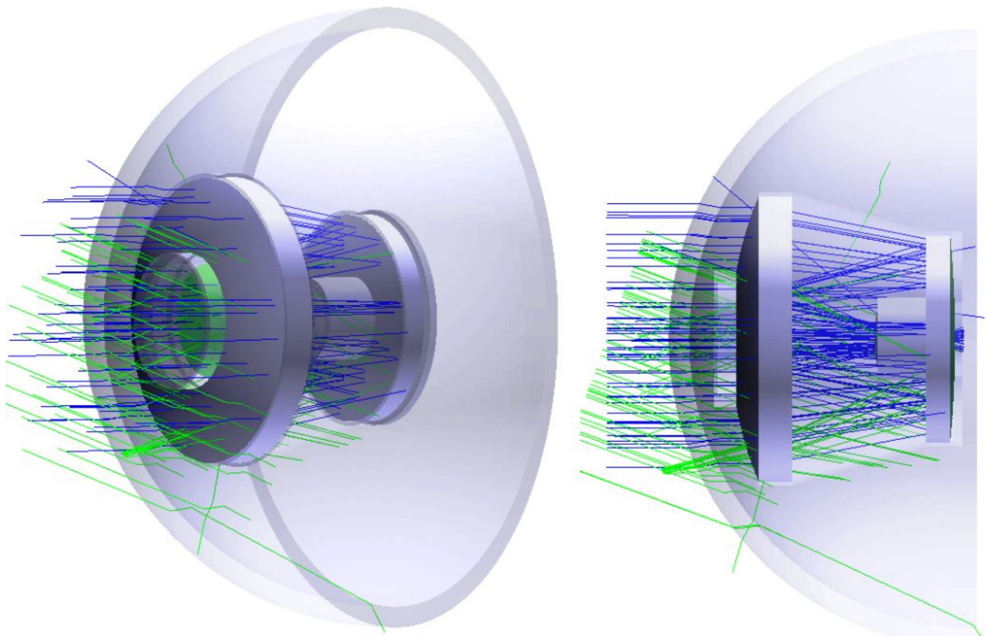

Fig. 10. Stray light models for the catadioptric system

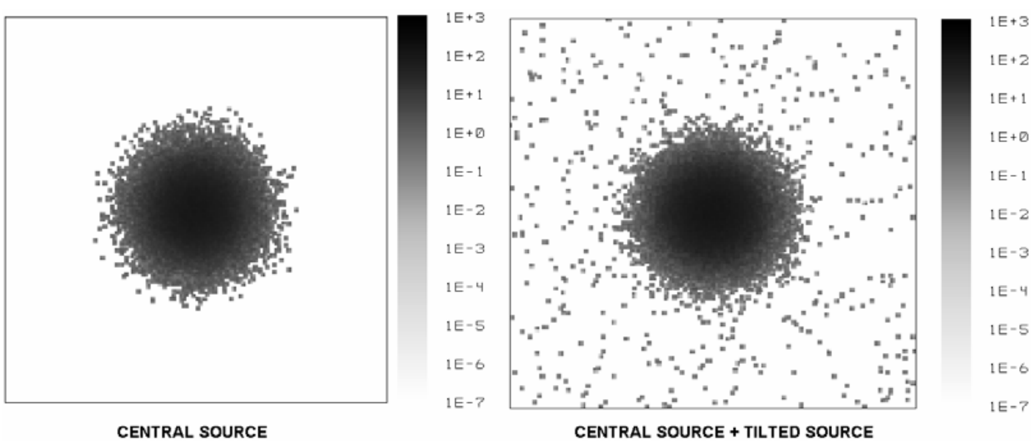

Fig. 11. Results for the catadioptric stray light model

5.2. Stray light analyses for the dioptric system

Once more, the requirements for the dioptric system are the same. The model will also be implemented using non-sequential mode and the FPA will be fully modeled. Figure 12 illustrates the dioptric model used for the stray light simulation.

For this dioptric system, it is possible to observe in Figure 13 that when the two sources are simulated, a part of the tilted source can be observed. This can be critical if the tilted source is more powerful (like a flare) than the central source (that could be the target). Consequently, for this dioptric system, the ability to reject stray light is seriously compromised and that should be considered as a risk for the system performance.

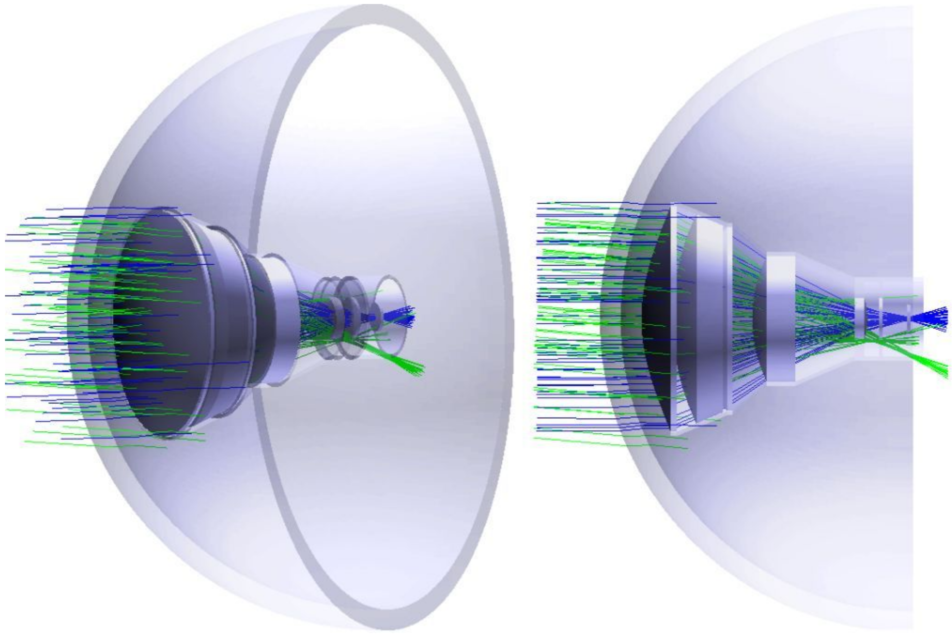

Fig. 12. Stray light models for the dioptric system.

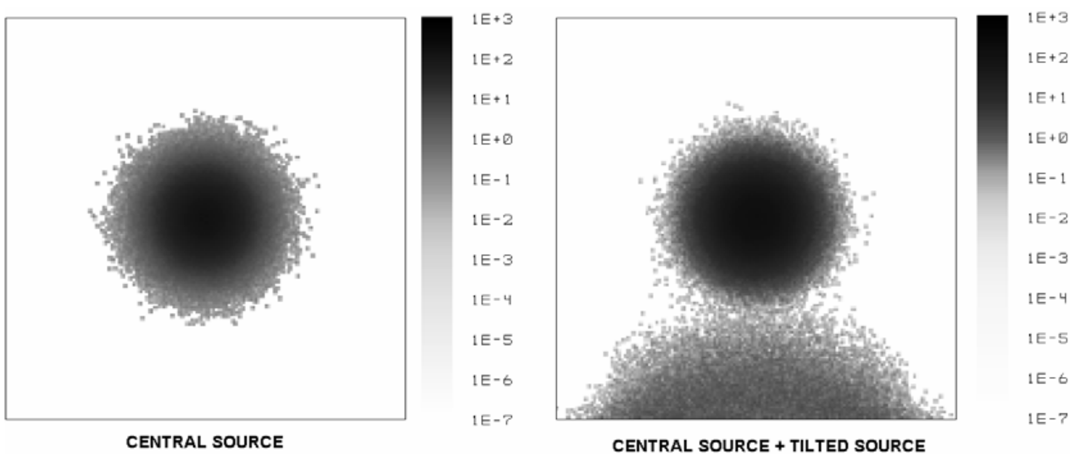

Fig. 13. Results for the dioptric stray light model

6. Systems Classification

After all the analyses have been done, it is possible to classify both systems accordingly to their characteristics of performance, weight, size, viability and price.

In terms of performance, both systems were accomplishing the requirements in terms of ensquared energy and athermalization. However, when the stray light analysis was concluded, it was clear that the dioptric system would not be able to reject stray light at 5^0 away from the IFOV. The stray light rejection is a crucial factor for this design and just for itself it is able to determine whether a system can be accepted or not. Consequently, as the dioptric system failed the stray light analysis, it cannot be used to compose the missile.

In terms of weight and size, both systems are very similar. Although the weight and size are parameters that can be decisive in the choice of the optical system, for this comparison they are not the most important, due to the similarity between the systems.

About viability, a catadioptric system using a Cassegrain is the well known classic solution. It is reasonably simple to assemble; the thermal and optical compensators are easy installed and the system provides a very good optical performance. A dioptric solution like the one presented in this paper may be extremely difficult to implement due to larger number of optical components.

Finally, comparing the prices, the catadioptric solution is cheaper due to the more common choice of materials. Cleartran® and CaF_2 are not cheap, but they are easily found and very good to be machined. Materials like CdSe and MgO are extremely expensive and not easy to purchase.

Summarizing all the comments, Table 2 illustrates the systems overall for all the requirements.

Table 2. Summary and classification for both optical systems

Optical system	Performance			Weight	Viability	Price
	Energy	Athermalization.	Stray Light			
Catadioptric	**Excellent**	**Excellent**	**Good**	**Heavy**	**Viable Well known**	**High**
Dioptric	**Very Good**	**Very good**	**Poor**	**Heavy**	**Difficult to assemble**	**Very high**

Therefore, after all these exhaustive analyses, it is possible to conclude that the classic solution, using a catadioptric Cassegrain modified is the most recommended due to its characteristics of performance, viability and price and eventually will integrate the optical system for this 5th generation air-to-air missile.

7. References

Kryszczyn´ski, T., Les´niewski, M., "Material problem in athermalization of optical systems", Opt. Eng. 36(6) 1596–1601 (June 1997).
Tamagawa, Y., Tajime, T., "Expansion of an athermal chart into a multilens system with thick lenses spaced apart", Opt. Eng. 35(10) 3001–3006 (October 1996).
Leite, P.R., Silva, M.G., "The influence of aerodynamic heating at the optical performance of missiles", Proceedings of ENCIT 2008.
Boshuizen, C. R. et al, " MONS space telescope, part 2: analysis of very high stray-light rejection", Optical Engineering, January 2008/Vol. 47_1_
Leite, P.R., Silva, M.G., Paoli, Eduardo T. “Design of an optical system for a 5th generation, multi-spectral, air-to-air missile, considering the imaging performance degradation due to the aerodynamic heating”, SPIE Defense, Security and Sensing, April 2009, 7338-21

8. Copyright Notice